Crystalline Phases

International Edition: DOI: 10.1002/anie.201604915
German Edition: DOI: 10.1002/ange.201604915

From Sponges to Nanotubes: A Change of Nanocrystal Morphology for Acute-Angle Bent-Core Molecules

Ewa Gorecka, Nataša Vaupotič, Anna Zep, and Damian Pociecha*

Abstract: *The crystalline (B_4) phase made of acute-angle bent-core molecules (1,7-naphthalene derivatives), which exhibits an unusual, highly porous sponge-like morphology, is presented. However, if grown in the presence of low-weight mesogenic molecules, the same crystal forms nanotubes with a very high aspect ratio. The nanotubes become unstable upon increasing the amount of dopant molecules, and the sponge-like morphology reappears. The phase is optically active, and the optical activity is an order of magnitude smaller than in the B_4 phase made of conventional bent-core molecules. The optical activity is related to the spatial inhomogeneity of the layered structure and is reduced due to the low apex angle and low tilt of the molecules. The arrangement of molecules within the layers was deduced from the bathochromic absorption shift in the B_4 phase.*

The equilibrium morphology of a crystal reflects its internal structure and is determined by the velocity at which the crystal walls grow. However, in nature, there exist crystals exhibiting unusual shapes that are not related to their internal structure. Biogenic crystals are often strongly curved with the zero mean surface curvature and large porosity. Such a morphology provides optimal mechanical strength and good solvent permeability. A perfect example is a bicontinuous sponge-like morphology of the sea urchin spines and skeletal plates.[1] Several complex biological mechanisms were proposed for being responsible for controlling the biogenic crystal morphology, for example, a special localization of minerals in the living species and crystal growth in confined geometries.[2] There are also artificial bioinspired crystalline materials with complex curved surfaces that were obtained by a templating procedure, using, for example, a diblock polymer or liquid-crystalline matrices.[3] Recently, it was shown that some organic mesogenic compounds spontaneously crystallize in strongly curved forms.[4,5] Bent-core mesogens can form membranes made of few molecular layers (in the liquid-crystal research, such a crystal is named a B_4 phase), that easily twist into ribbons. It seems that this morphology dominates in the B_4 phase, irrespective of how the material crystallizes (in bulk, under confinement, or in solvents),[6,7] the other morphologies like nanotubes are only rarely reported.[8] The mechanism proposed for being responsible for the twisting is the incompatibility between the volume required by the molecular cores and alkyl chains.[4]

A similar mechanism is also well-known on the macroscale; the most famous examples are the potato chips that adopt their shape when the potato disk edges shrink faster than the disk bulk, or some plant leafs that show an excess growth in marginal regions.[9]

Herein we present materials that crystallize into a highly porous, local gyroid structure under the ambient conditions, without an addition of precursors and/or templating procedure. If the crystallization takes place in the presence of a small amount of a liquid-crystalline solvent (nematic or smectic), the morphology of nanocrystals changes and nanotubes are formed instead of a gyroid phase.

The studied materials are bent-core mesogens with an acute angle between the molecular arms, defined by the 1,7-substitution of the central naphthalene ring (Figure 1). The compounds were synthesized according to the previously

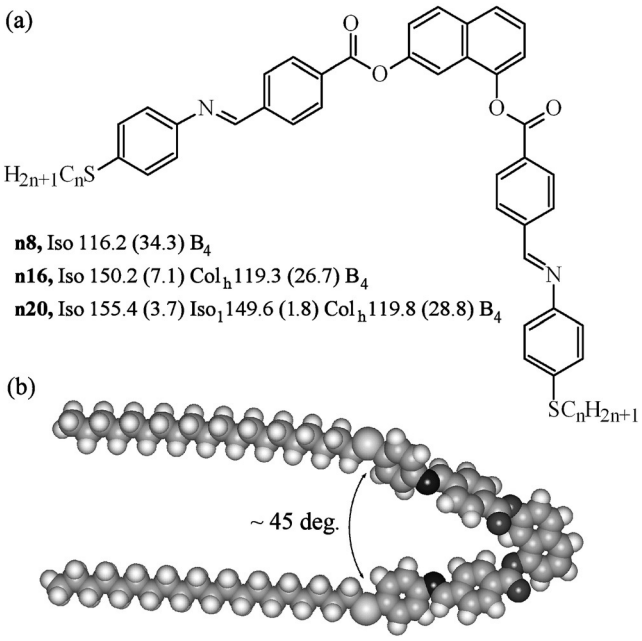

Figure 1. Molecular structure and the phase transition temperatures (in °C) and enthalpy changes (in parentheses, $J g^{-1}$) obtained on cooling (10 K min^{-1}) for the studied compounds. Iso and Iso_1: optically isotropic liquids, Col_h -2D columnar hexagonal phase, B_4: lamellar crystal phase.

[*] Prof. E. Gorecka, A. Zep, Dr. D. Pociecha
University of Warsaw, Department of Chemistry
ul. Żwirki i Wigury 101, 02-089 Warsaw (Poland)
E-mail: gorecka@chem.uw.edu.pl
Prof. N. Vaupotič
Department of Physics
Faculty of Natural Sciences and Mathematics
University of Maribor, Koroška 160, 2000 Maribor (Slovenia)
and
Jozef Stefan Institute
Jamova 39, 1000 Ljubljana (Slovenia)

Supporting information for this article can be found under: http://dx.doi.org/10.1002/anie.201604915.

described procedure.[10] The phase sequence was identified as: Iso-B_4 for **n8**, Iso-Col_h-B_4 for **n16**, and Iso-Iso_1-Col_h-B_4 for **n20**. The Iso_1 phase is an optically isotropic liquid; its X-ray diffraction (XRD) pattern with no Bragg-type reflections is typical for phases with only a short-range positional order. The position of the diffused low-angle diffraction signal coincides with the position of the most intensive signal of the Col_h phase formed below the Iso_1 phase (Supporting Information, Figure S1), so we conclude that the Iso_1 phase is built of columnar-like molecular assemblies with the short-range positional and orientational correlations.

The XRD pattern of the columnar phase shows a series of sharp reflections in the small angle range with the ratio of the positions in the q-space being $1:\sqrt{3}:2$, which is characteristic for the 2D hexagonal arrangement of columns, Col_h. The diffused signal at high angles indicates the liquid-like positional correlations along the columns. From the measured column diameter ($a = 7.0$ and 7.4 nm for **n16** and **n20**, respectively) and assuming the density of material 1 g cm^{-3}, it is estimated that the column cross-section is built of approximately 8 to 10 molecules. Watanabe et al.[11] argued that the column cross-section is made of strongly bent smectic layers; however, it should be stressed that such a model of the columnar phase imposes a very different density of alkyl chains inside and outside the column stratum filled with aromatic parts of molecules. Thus, an alternative model should also be considered, proposed previously for the polycatenar bent-core molecules,[12] according to which molecules are arranged into disk-like aggregates. A large number of molecules in the column cross-section requires the molecular conformation with a small angle between the molecular arms (ca. 40°), which is possible for the studied molecules by adopting proper dihedral angles on ester linkages (Figure 1b).

For the temperature-quenched samples, several diffraction signals in the low- and high-angle regions of the XRD pattern are observed (Figure 2), indicating a crystalline structure of the phase at room temperature.

The signals are significantly broadened due to the finite size of the nanocrystallites, as usually observed for the B_4 phase.[13] The commensurability of the low-angle diffraction signals confirms a lamellar-type local crystallographic structure with the layer thickness d (for compound **n20** $d \approx 4.4$ nm, for **n16** $d \approx 3.9$ nm, and for **n8** $d \approx 2.8$ nm) corresponding roughly to the molecular length measured from the naphthalene apex to the end of the alkyl chain, or to the distance between the ends of the alkyl chains for the molecules with a 50–60° opening angle between the arms. The layer thickness is nearly constant in the whole temperature range of the B_4 phase. On heating, some samples show a sequence of a crystal-crystal phase transitions above the B_4 phase, before melting to the Col_h phase, which indicates a metastable character of the B_4 phase.

Optically, the transition from the Col_h to the B_4 phase is accompanied by a sudden lowering of birefringence, which suggests a space averaging of molecular orientations; however, in most samples neither optically active domains nor a circular dichroism (CD) signal, which are characteristic for the B_4 phase,[14] were detected. The gelation ability, commonly observed for the B_4 materials,[15] was very weak for the studied compounds. They showed good solubility in most non-polar organic solvents (such as hexane, cyclohexane) at elevated temperature, but precipitated at room temperature; in polar solvents (ethanol, methanol) the compounds were not soluble; among the tested solvents a weak gel was formed only in toluene.

To obtain additional information on the arrangement of molecules and molecular interactions, the UV/Vis absorption studies were performed as a function of temperature for compound **n20** (Figure 3; Supporting Information, Figure S2). The observed strong absorption band is due to the presence of the benzylideneaniline units in the molecular arms. The absorption measured in the B_4 phase ($\lambda_{max} = 368$ nm) showed a small bathochromic shift compared to the absorption of isolated molecules in a non-polar solvent ($\lambda_{max} = 366$ nm in the toluene), while in Col_h phase a hypsochromic shift was observed ($\lambda_{max} = 354$ nm). This clearly indicates that the nearest-neighbor interactions of molecules in the Col_h and B_4 phases are different.

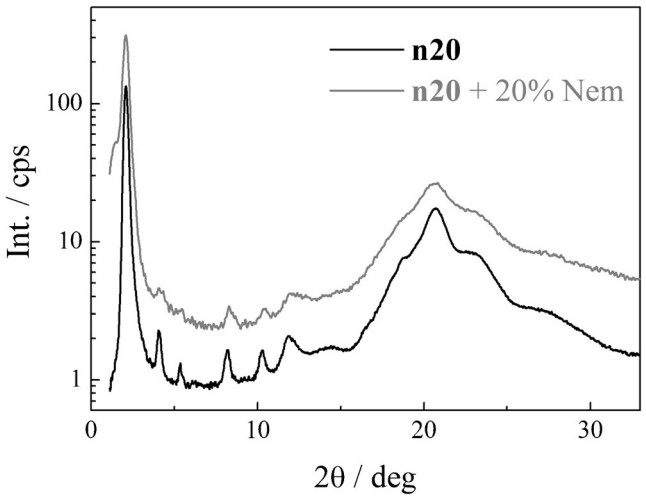

Figure 2. X-ray diffraction patterns for the B_4 phase of a pure compound **n20** (black line) and its mixture with 20 wt% of nematogen (gray line).

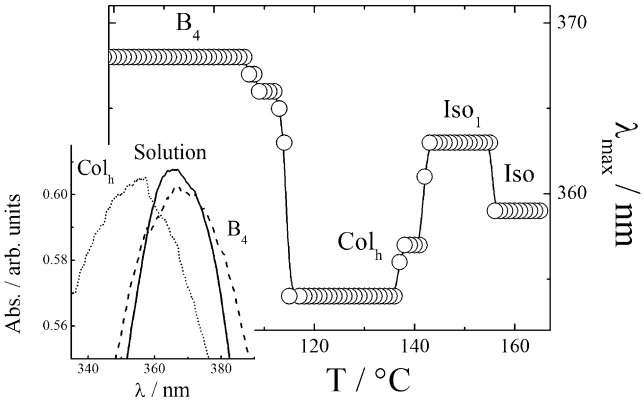

Figure 3. Absorption maximum wavelength measured on cooling for compound **n20**. Inset: an enlarged part of absorption spectra recorded in the Col_h and B_4 phases and for the solution in toluene.

To reveal the molecular packing in the columnar phase, a crude estimation of the energy shift due to the transitional dipole–dipole interactions was performed for the two possible arrangements of molecules in the column cross-section (Figure 4a,b). It is known that a parallel arrangement of the interacting transition dipoles (H-aggregates) increases the energy level of the excited state, which results in a blue-shift of absorption, while a head-to-tail arrangement (J-aggregates) results in lowering of the excited state energy and thus a red-shift. However, the exact value and sign of the energy shift depends on the relative position and orientation of the dipoles. Considering the molecular arrangements presented in Figure 4 it was estimated (see the Supporting Information) that the dipole–dipole interaction energy is positive for the radial orientation of dipoles (Figure 4a) and negative for the dipoles oriented tangentially (Figure 4b). Including the contribution of the dipoles in the column stratum above/below [see Eq. (1) in the Supporting Information] does not change the sign of the interaction energy. Because a hypsochromic shift was observed in the columnar phase ($\Delta\lambda = -12$ nm), it can be concluded that the dipoles in the column cross-section are oriented radially, as shown in Figure 4a. For the distance between the neighboring column cross-sections equal to 0.4 nm and the radius of the circle over which the dipoles are distributed equal to 1.5 nm, the model gives the total interaction energy of the radially distributed dipoles:

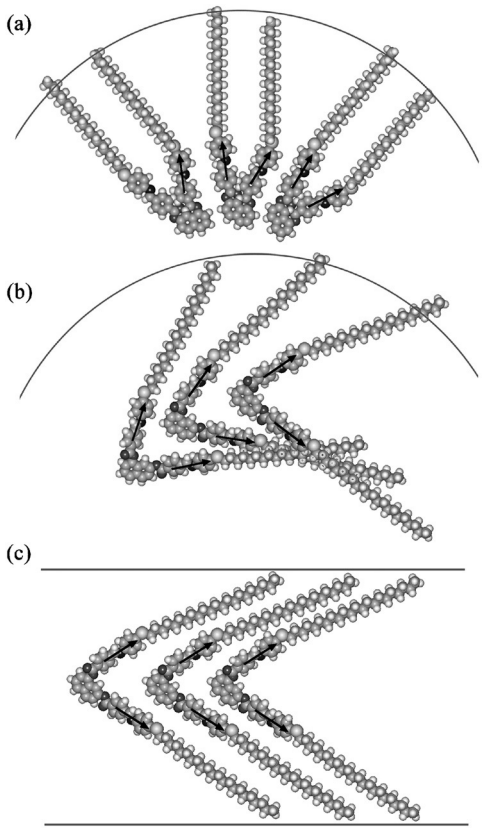

Figure 4. Possible arrangement of molecules in the Col_h phase: a) radial and b) tangential and c) in the B_4 phase. Arrows indicate the transition dipole moments of the benzylideneaniline units.

$$E_{int}^{(Col)} = 100\,E_0, \text{ where } E_0 = \frac{\mu^2}{4\pi\,\varepsilon_0\,{r_0}^3}$$

with μ denoting the magnitude of the induced dipole and $r_0 =$ 1.0 nm. Accordingly, the measured energy shift $\Delta E = 0.11$ eV corresponds to the transition dipole moment $\mu = (1.3 \pm 0.1)$ D, an experimental error of ± 1 nm in the wavelength shift was considered for calculating the uncertainty of μ.

On the other hand, the bathochromic shift observed in the B_4 phase suggests that the layers are made of molecules arranged tangentially, with their apexes in the mid-plane of the layer (Figure 4c). The magnitude and sign of the resulting interaction energy depends strongly on the inclination of dipoles, and thus on the apex angle of the molecule. The interaction energy is positive for large apex angles (for example, typical bent-core molecules with the apex angle of 120°),[16] and it becomes negative for molecules with an acute angle ($< 58°$, see the Supporting Information). By ignoring a small tilt of molecules from the layer normal and taking the apex angle of 36° (the same as in the columnar phase), the distance between the dipoles in the same molecule as 0.4 nm and the in-plane distances between the neighboring molecules in the orthorhombic unit cell as $r_{01} = 1.0$ nm and $r_{02} = 0.5$ nm, $E_{int}^{(B4)} = -25\,E_0$ is obtained. The measured energy shift $\Delta E = -0.019$ eV then corresponds to $\mu = (1.2 \pm 0.1)$ D. Assuming the apex angle equal 50°, which is more consistent with the X-ray data, the calculated dipole moment increases to (1.8 ± 0.5) D. The model of the molecular arrangement in the layers of the B_4 phase (Figure 4c) is consistent with the electron density profile deduced from the X-ray data (Supporting Information, Figure S3). The elongation of the alkyl chains broadens the low density regions while the width of the higher density regions, filled with the aromatic parts, remains nearly constant, approximately 1.7 nm. A similar value of the mesogenic core length is obtained by the extrapolation of the layer spacing dependence on the number of carbon atoms in the terminal chains to $n = 0$ (Supporting Information, Figure S4); moreover the inclination of the $d(n)$ dependence yields the apex angle close to 50°, assuming a small tilt angle of few degrees.

The AFM studies for the thin (1–2 μm) B_4 samples, quenched from the isotropic phase to the room temperature revealed bamboo-like features, which are related to the torrical focal-conic domains (TCFD), built of units being approximately 35 nm wide and 70 nm long (Figure 5a). For thicker samples the distorted network of interconnected objects with multiple nodes becomes visible (Figure 5b); the diameter of rods and their persistent length are similar to those observed for the bamboo-like units in thin samples. Locally, the structure strongly resembles the distorted bicontinuous cubic phases.[17]

The morphology of the nanocrystals changes substantially if compounds (**n16** or **n20)** recrystallize in the presence of a low-molecular-weight nematogen or smectogen (see the Supporting Information). An addition of more than 10 wt% of a nematic material completely destabilizes the Col_h phase and the B_4 phase grows directly from the isotropic melt. The X-ray diffraction pattern of the B_4 phase grown in the presence of the nematogen is identical (Figure 2) to that of

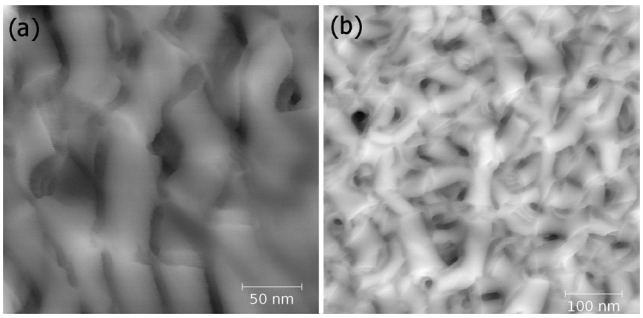

Figure 5. AFM image of the bamboo-like structures observed in a a) thin and b) thick sample of compound **n20**.

the pure material, despite of the fact that the local morphology strongly depends on the nematogen concentration. For the mixtures with approximately 20 wt% of the nematic compound, hollow tubules were formed by wrapped layers (Figure 6). Nanotubes are nearly homogenous in diameter (ca. 70–80 nm), with the inner hole of approximately 20 nm; the walls of tubules are made of approximately 7 layers. The tubules have a large aspect ratio; their length reaches few μm (Figure 6). The weak shearing of the sample at the Iso-B_4 phase transition resulted in a uniform grow of the nanotubes, perpendicular to the sample surface in a large, μm-sized areas (Supporting Information, Figure S5). Upon increasing the content of the nematogenic molecules in the mixture, the tubules become unstable. Perforated membranes with a locally negative curvature and large and non-regular pores are formed (Figure 6d).

We propose the following explanation for the observed structural transitions. In the sponge-like structure, the surfaces with positive and negative splay offer only a small possibility for the dopant molecules to adsorb. The outer surface of tubules have uniform positive curvature and the positive molecular splay that facilitates the penetration of the dopant molecules into the membrane surface. An increase in the number of dopant molecules that are adsorbed at the B_4 membrane leads to a change of the preferred curvature of the membrane from the local saddle-splay to cylindrical. When the number of nematogenic molecules becomes large enough, the system prefers to form separated areas occupied with the dopant molecules in the energetically preferred sponge-like structure of studied compound, which results in the morphology shown in Figure 6d.

The formation of nanotubes is not unique for the chosen nematogen. An addition of a smectogen material (see the Supporting Information) also causes the formation of nanotubes, but for this system nanotubes usually co-exist with flat crystal plates (Figure 7), the tubules are usually formed at the plate edges. It seems that in this case, the energies of the flat layers and nanoobjects with the zero Gaussian curvature are very similar.

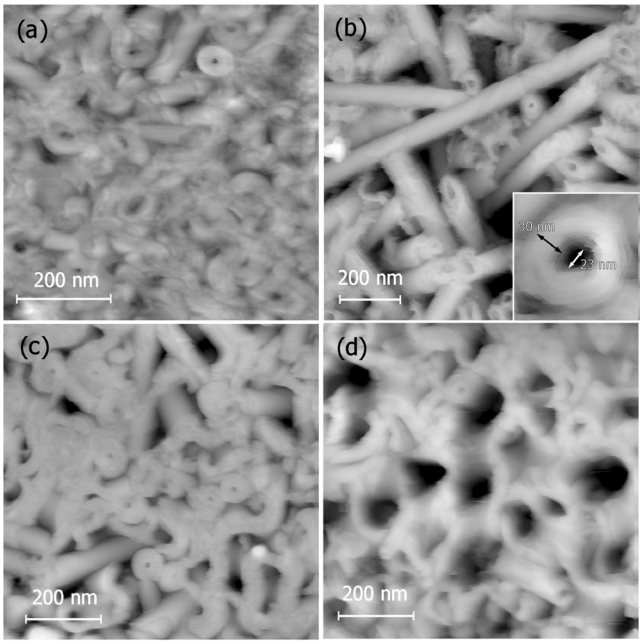

Figure 6. AFM images showing the changes of the crystal morphology for compound **n16** upon doping with a) 10 wt%, b) 20 wt%, c) 23 wt%, and d) 30 wt% of the nematic material. Inset to b): the tubule cross-section.

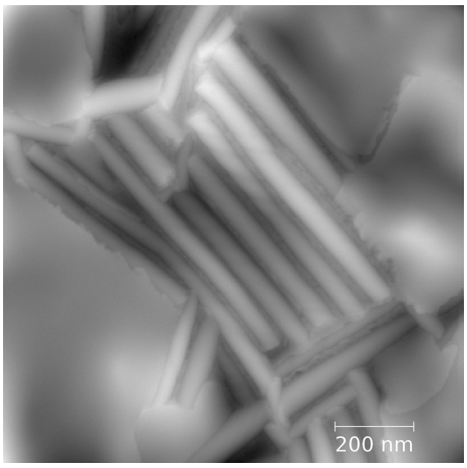

Figure 7. AFM image showing the coexistence of flat sheets and nanotubes of compound **n16** doped with 20 wt% of a smectic material.

Interestingly, while for the pure material the B_4 phase grown from the Col_h phase is usually not optically active, the samples contaminated by a small amount of a mesogenic compound or isotropic solvent form optically active domains (Supporting Information, Figure S6), that grew from a single nucleation site. Thus, the additives enhance the chiral segregation. By analogy to cancellation of chirality in the $Ia\bar{3}d$ cubic phase,[18] the lack of the optical activity of the B_4 phase grown from the Col_h phase suggests that the sponge-like structure is a double gyroid (bicontinuous) structure built of two interpenetrating networks having the opposite sign of the layer chirality. The transition to the tubular structure removes this intrinsically conglomerated structure.

The optical rotatory power (ORP) of approximately $0.1° \mu m^{-1}$ and $0.05° \mu m^{-1}$ for **n8** and **n20,** respectively was nearly independent on the concentration of the additive. The measured ORP is 2–3 times smaller than the value reported for the B_4 phases of conventional bent-core materials with a 120° apex angle.[19] The optical activity was observed also for

samples built from flat crystal plates, which means that the optical activity is not related to the formation of tubes or a sponge-like nanoobjects but to the arrangement of the bent-core molecules in the crystal lattice. Among 32 crystallographic classes, 15 have gyration tensors with non-zero elements, allowing optical activity;[20] among them there are 4 non-enantiomorphous classes (point groups: *m*, *mm*2, $\bar{4}$ and $\bar{4}2m$) with the axial gyration tensor corresponding to the 4*m* symmetry, leading to the ORP cancelation in the powder crystal samples, which is in disagreement with the experimental results. Among the remaining 11 enantiomorphous classes the most relevant for the B_4 structure are the point groups 1 and 2 that require molecules in a single layer to be tilted from the layer normal and having a uniform orientation inside the layer. Adopting the model based on spatial inhomogeneity of the dielectric tensor of a crystal layer[21] (see the Supporting Information), we estimated that the measured value of the ORP (ca. $0.1° \mu m^{-1}$) for the crystal isostructured with the ferroelectric synclinic smectic C phase ($SmCsP_F$) built of acute angle molecules corresponds to the tilt of approximately few degrees. As in conventional bent-core molecules, the layer chirality and the resulting optical activity depend on the molecular tilt with respect to the layer normal and molecular tip direction.

Summarizing, we have shown that the acute-angle molecules of the 1,7-naphthalene derivatives form the B_4 crystalline phase with layers made of molecules that are arranged tangentially with their apexes in the mid-plane, and a columnar phase in which molecules are arranged radially in the column stratum. The different arrangement of molecules in the Col_h and B_4 phases and therefore different interactions of the transitional dipoles of the benzylideneaniline units in the molecular arms result in a shift of absorption maxima, hypsochromic in the Col_h phase and bathochromic in the B_4 phase. Contrary to the conventional B_4 materials, helical nanofilaments were not formed.[4,7,14,22] Instead, the local sponge-like morphology was observed for the pure materials in the B_4 phase. In a narrow concentration window of the nematogenic or smectogenic additives, homogenous nanotubules with high aspect ratio were observed. We have confirmed that the optical activity of the B_4 phase is related to its crystalline structure. For the acute-angle molecules, assuming a small tilt of molecules from the layer normal, the model predicts much lower optical activity than for the ordinary bent-core materials, which agrees with our experimental observations. The studied compounds belong to rare class of achiral materials forming chiral crystal structures.[23]

Acknowledgements

The research was financed by the project NCN DEC-2012/07/B/ST5/02448 and the research program P1-0055 of the Slovenian Research Agency. Authors thank Prof. Mojca Čepič and Prof. Hideo Takezoe for valuable discussions.

Keywords: bent-core materials · nanotubes · optical activity · sponge phase

How to cite: *Angew. Chem. Int. Ed.* **2016**, *55*, 12238–12242
Angew. Chem. **2016**, *128*, 12426–12430

[1] X. Su, S. Kamat, A. H. Heuer, *J. Mater. Sci.* **2000**, *35*, 5545–5551.
[2] F. C. Meldrum, *Int. Mater. Rev.* **2003**, *48*, 187–224.
[3] W. Yue, A. N. Kulak, F. C. Meldrum, *J. Mater. Chem.* **2006**, *16*, 408–416.
[4] L. E. Hough, H. T. Jung, D. Krüerke, M. S. Heberling, M. Nakata, C. D. Jones, D. Chen, D. R. Link, J. Zasadzinski, G. Heppke, J. P. Rabe, W. Stocker, E. Körblova, D. M. Walba, M. A. Glaser, N. A. Clark, *Science* **2009**, *325*, 456–460.
[5] D. Chen, M. S. Heberling, M. Nakata, L. E. Hough, J. E. Maclennan, M. A. Glaser, E. Körblova, D. M. Walba, J. Watanabe, N. A. Clark, *ChemPhysChem* **2012**, *13*, 155–159.
[6] S. Lee, H. Kim, E. Tsai, J. M. Richardson, E. Korblova, D. M. Walba, N. A. Clark, S. B. Lee, D. K. Yoon, *Langmuir* **2015**, *31*, 8156–8161.
[7] J. Matraszek, N. Topnani, N. Vaupotič, H. Takezoe, J. Mieczkowski, D. Pociecha, E. Gorecka, *Angew. Chem. Int. Ed.* **2016**, *55*, 3468–3472; *Angew. Chem.* **2016**, *128*, 3529–3533.
[8] K. V. Le, F. Araoka, *Abstract Book of the 15th International Conference on Ferroelectric Liquid Crystals*, **2015**, p. 82; *Abstract Book of TOYOTA RIKEN International Workshop on Bent-Core Liquid Crystals*, **2015**, p. 42.
[9] a) R. D. Kamien, *Science* **2007**, *315*, 1083–1084; b) Y. Klein, E. Efrati, E. Sharon, *Science* **2007**, *315*, 1116–1120; c) S. Armon, O. Yanai, N. Ori, E. Sharon, *J. Exp. Bot.* **2014**, *65*, 2071–2077.
[10] S. Kang, M. Harada, M. Tokita, J. Watanabe, *Soft Matter* **2012**, *8*, 1916–1922.
[11] S. Kang, X. Li, S. Kawauchi, X. Li, M. Tokita, J. Watanabe, *Mol. Cryst. Liq. Cryst.* **2011**, *549*, 184–193.
[12] E. Gorecka, D. Pociecha, J. Mieczkowski, J. Matraszek, D. Guillon, B. Donnio, *J. Am. Chem. Soc.* **2004**, *126*, 15946–15947.
[13] E. Białecka-Florjańczyk, I. Śledzińska, E. Górecka, J. Przedmojski, *Liq. Cryst.* **2008**, *35*, 401–406.
[14] D. Chen, J. E. Maclennan, R. Shao, D. K. Yoon, H. Wang, E. Korblova, D. M. Walba, M. A. Glaser, N. A. Clark, *J. Am. Chem. Soc.* **2011**, *133*, 12656–12663.
[15] A. Zep, M. Salamonczyk, N. Vaupotič, D. Pociecha, E. Gorecka, *Chem. Commun.* **2013**, *49*, 3119–3121.
[16] F. Araoka, T. Otani, K. Ishikawa, H. Takezoe, *Phys. Rev. E* **2010**, *82*, 041708.
[17] L. E. Hough, M. Spannuth, M. Nakata, D. A. Coleman, C. D. Jones, G. Dantlgraber, N. A. Clark, *Science* **2009**, *325*, 452–456.
[18] C. Dressel, F. Liu, M. Prem, X. Zeng, G. Ungar, C. Tschierske, *Angew. Chem. Int. Ed.* **2014**, *53*, 13115–13120; *Angew. Chem.* **2014**, *126*, 13331–13336.
[19] F. Araoka, G. Sugiyama, K. Ishikawa, H. Takezoe, *Opt. Mater. Express* **2011**, *1*, 27–35.
[20] R. Gautier, J. M. Klingsporn, R. P. van Duyne, K. P. Poeppelmeier, *Nat. Mater.* **2016**, *15*, 591–592.
[21] L. E. Hough, N. A. Clark, *Phys. Rev. Lett.* **2005**, *95*, 107802.
[22] T. Ueda, S. Masuko, F. Araoka, K. Ishikawa, H. Takezoe, *Angew. Chem. Int. Ed.* **2013**, *52*, 6863–6866; *Angew. Chem.* **2013**, *125*, 7001–7004.
[23] C. Tschierske, G. Ungar, *ChemPhysChem* **2016**, *17*, 9–26.

Received: May 19, 2016
Revised: July 18, 2016
Published online: September 5, 2016

